Neuron

High Salt Intake Increases Blood Pressure via BDNF-Mediated Downregulation of KCC2 and Impaired Baroreflex Inhibition of Vasopressin Neurons

Highlights

- Chronic high salt intake reduces chloride gradient in vasopressin neurons

- BDNF-TrkB activation causes KCC2 downregulation and collapse of chloride gradient

- High salt intake abolishes baroreceptor inhibition of vasopressin neurons

- Circulating vasopressin mediates high blood pressure during high salt intake

Authors

Katrina Y. Choe, Su Y. Han, ...,
J. Thomas Cunningham,
Charles W. Bourque

Correspondence

charles.bourque@mcgill.ca

In Brief

High salt consumption is causally linked to hypertension with unclear etiology. Choe et al. show that chronic high salt modifies a hypothalamic circuit, leading to excessive release of the antidiuretic hormone vasopressin. The resulting peripheral vasoconstriction increases blood pressure.

CellPress

Neuron

Article

High Salt Intake Increases Blood Pressure via BDNF-Mediated Downregulation of KCC2 and Impaired Baroreflex Inhibition of Vasopressin Neurons

Katrina Y. Choe,[1] Su Y. Han,[2] Perrine Gaub,[3] Brent Shell,[4] Daniel L. Voisin,[5] Blayne A. Knapp,[4] Philip A. Barker,[3] Colin H. Brown,[2] J. Thomas Cunningham,[4] and Charles W. Bourque[1,*]
[1]Centre for Research in Neuroscience, Research Institute of the McGill University Health Centre, 1650 Cedar Avenue, Montreal, QC H3G1A4, Canada
[2]Centre for Neuroendocrinology and Department of Physiology, University of Otago, Dunedin 9054, New Zealand
[3]Montreal Neurological Institute, 3801 University Street, Montreal, QC H3A2B4, Canada
[4]Department of Integrative Physiology, University of North Texas Health Sciences Centre, 3500 Camp Bowie Boulevard, Fort Worth, TX 76107, USA
[5]Neurocentre Magendie, INSERM U862, 146, rue Léo Saignat, 33077 Bordeaux, France
*Correspondence: charles.bourque@mcgill.ca
http://dx.doi.org/10.1016/j.neuron.2014.12.048

SUMMARY

The mechanisms by which dietary salt promotes hypertension are unknown. Previous work established that plasma [Na$^+$] and osmolality rise in proportion with salt intake and thus promote release of vasopressin (VP) from the neurohypophysis. Although high levels of circulating VP can increase blood pressure, this effect is normally prevented by a potent GABAergic inhibition of VP neurons by aortic baroreceptors. Here we show that chronic high salt intake impairs baroreceptor inhibition of rat VP neurons through a brain-derived neurotrophic factor (BDNF)-dependent activation of TrkB receptors and downregulation of KCC2 expression, which prevents inhibitory GABAergic signaling. We show that high salt intake increases the spontaneous firing rate of VP neurons in vivo and that circulating VP contributes significantly to the elevation of arterial pressure under these conditions. These results provide the first demonstration that dietary salt can affect blood pressure through neurotrophin-induced plasticity in a central homeostatic circuit.

INTRODUCTION

High levels of dietary salt intake can significantly increase plasma sodium concentration and contribute to the development of salt-dependent hypertension (He et al., 2013; He and Macgregor, 2012; Schmidlin et al., 2007). However, the central mechanisms by which excess sodium can increase blood pressure (BP) remain poorly defined. Previous work has shown that a rise in plasma sodium can excite hypothalamic magnocellular neurosecretory cells (MNCs) that release the antidiuretic and vasoconstrictor hormone vasopressin (VP) (Bourque, 2008; Voisin and Bourque, 2002). Although VP can enhance BP when infused systemically (Fujiwara et al., 2012), increases in BP normally activate arterial baroreceptors (BR) that inhibit VP MNCs via GABA$_A$ receptors (GABA$_A$R) (Cunningham et al., 2002; Renaud et al., 1988). In principle, this negative feedback regulation of MNCs should mitigate the involvement of circulating VP in the development of hypertension. However, a recent study has shown that rat MNCs display a collapse in the transmembrane chloride (Cl$^-$) gradient required for inhibitory GABA$_A$R signaling after chronic salt loading (Kim et al., 2011). A similar effect can be induced by a high-salt diet in uni-nephrectomized rats treated with deoxycorticosterone acetate (DOCA), where a weakening of BR-mediated inhibition is also associated with a VP-dependent increase in BP (Kim et al., 2013). These observations indicate that plastic changes in the BR-mediated control of MNCs can allow these cells to participate in the regulation of BP. However, it remains unknown if high dietary salt intake can by itself mediate a VP-dependent form of hypertension, and the signaling mechanisms responsible for state-dependent changes in the BR-mediated control of VP MNCs are unknown.

Recent studies have shown that a weakening of GABA$_A$R-mediated inhibition caused by a collapsed Cl$^-$ gradient can emerge under several pathological conditions, including chronic pain (Coull et al., 2003), epilepsy (Huberfeld et al., 2007), stress (Hewitt et al., 2009), and spasticity following spinal cord injury (Boulenguez et al., 2010). In each instance experiments revealed that the effect was caused by a downregulation of the expression or activity of the K$^+$/Cl$^-$ co-transporter 2 (KCC2), a molecule that maintains the low levels of intracellular [Cl$^-$] required for inhibitory GABA$_A$R signaling (Ferrini and De Koninck, 2013). The expression of KCC2 is tightly linked to the activity of tropomyosin-related kinase B (TrkB) receptors, whose activation can suppress KCC2 transcription (Rivera et al., 2004). Although TrkB receptors can be activated by several ligands (McNamara and Scharfman, 2012; Yoshii and Constantine-Paton, 2010), recent studies have shown that the potent TrkB agonist brain-derived neurotrophic factor (BDNF) (Lu, 2003) is a common mediator of TrkB activation and KCC2 downregulation in central neurons (Boulenguez et al., 2010; Coull et al., 2005; Huang et al., 2013; Molinaro et al., 2009). Moreover, BDNF is highly expressed in
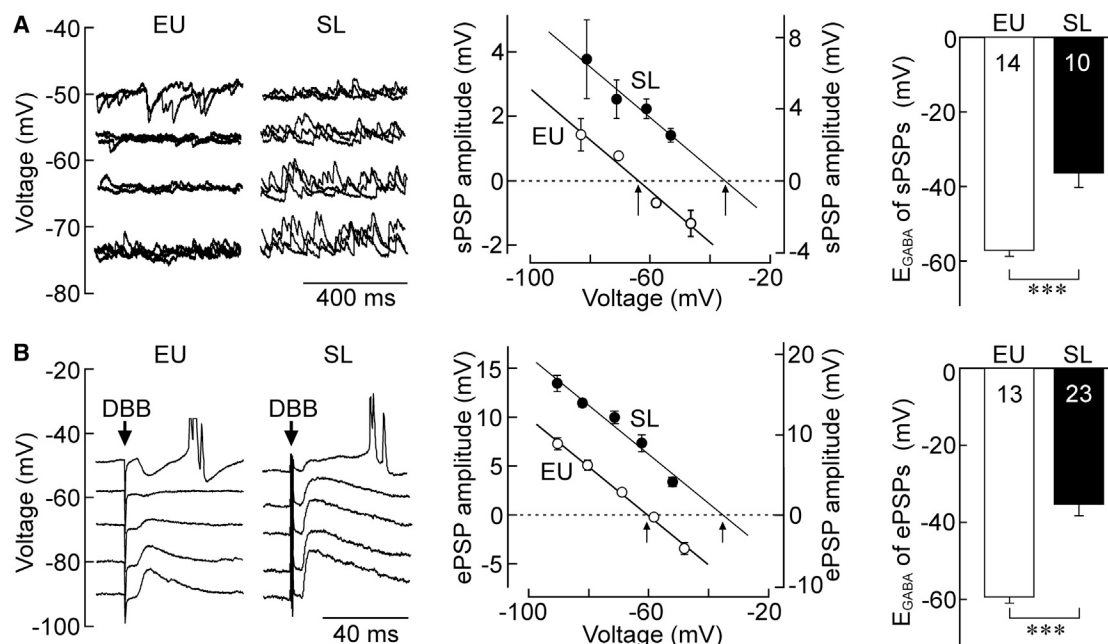
Figure 1. SL Shifts E_{GABA} in MNCs

(A) Sweeps at left show sPSPs recorded using sharp electrodes at various voltages from MNCs in explants prepared from EU and SL rats (see Figures S1 and S2). Plots in the middle panel show mean (± SEM) sPSP amplitude for the cells at left against baseline voltage (arrows show E_{REV}). Bar graphs at right represent the mean (± SEM) of all collected E_{GABA} values from sPSP analysis in all cells tested.

(B) Sweeps at left show PSPs evoked by electrical stimulation of the DBB at various voltages in MNCs recorded from EU and SL explants. Plots in the middle show mean (± SEM) evoked PSP (ePSP) amplitudes for cells at left against baseline voltage (arrows show E_{REV}). Bar graphs at right represent the mean (± SEM) of all E_{GABA} values determined from ePSP analysis (n shown on bars; ***p < 0.001).

VP MNCs (Aliaga et al., 2002; Arancibia et al., 2007; Castren et al., 1995), and in vivo experiments have shown that the dendrites of these neurons can release BDNF in response to electrical activity induced by a systemic increase in plasma [Na⁺] (Arancibia et al., 2007). In this study we therefore investigated whether chronic high dietary salt intake can provoke VP-dependent hypertension due to a BDNF-TrkB-KCC2-mediated weakening of BR inhibition of VP MNCs.

RESULTS

SL Depolarizes E_{GABA} and Eliminates Inhibitory Tone

To confirm that chronic high salt intake causes a collapse of Cl⁻ gradient in MNCs (Kim et al., 2011), we first examined the voltage dependence of GABA$_A$R-mediated postsynaptic potentials (PSPs) using sharp electrode intracellular recordings in hypothalamic explants prepared from euhydrated (EU) rats or animals provided with 2% NaCl as drinking solution for 7 days (SL; salt loading). This treatment resulted in a significant increase in plasma osmolality (Figure S1), as reported previously (Kim et al., 2011). Recordings were obtained from the VP-rich zone of the supraoptic nucleus (see Experimental Procedures), and DNQX (20 μM) was present to block fast ionotropic glutamatergic transmission. The average input resistances of recorded MNCs from EU and SL rats were 167.6 ± 14.8 MΩ (n = 27) and 116.6 ± 7.9 MΩ (n = 33), respectively (p = 0.0016). Spontaneous PSPs (sPSPs) recorded under these con-

ditions were completely eliminated by the addition of GABA$_A$R blockers bicuculline (10 μM; not shown) or gabazine (1 μM; Figure S2), confirming their dependence on these receptors. As illustrated in Figure 1A, GABA$_A$R-mediated sPSPs recorded in MNCs from EU preparations were consistently hyperpolarizing at voltages near action potential (AP) threshold (i.e., rheobase ∼−45 mV), reversing polarity at −57.2 ± 1.5 mV (n = 14, six rats). In contrast, sPSPs recorded in MNCs from SL preparations were generally depolarizing at voltages near AP threshold and reversed at −36.4 ± 3.9 mV; n = 10, three rats; p = 0.000012 versus EU control).

We next examined the value of E_{GABA} determined from the voltage dependence of PSPs evoked in MNCs by stimulation of the nucleus of the diagonal band of Broca (DBB), a site that relays the inhibitory effect of BRs onto VP MNCs in the supraoptic nucleus (Cunningham et al., 2002; Renaud et al., 1988). Electrical stimulation of the DBB caused prominent gabazine-sensitive PSPs in MNCs (Figure S2) and the average value of E_{GABA} determined from these responses was significantly more positive in explants prepared from SL rats (−35.3 ± 2.9 mV; n = 23, eight rats) than EU rats (−59.4 ± 1.6 mV; n = 13, seven rats; p = 0.0000015; Figure 1B). Identical results were obtained using gramicidin perforated patch recordings from identified VP neurons in angled hypothalamic slices prepared from transgenic Wistar rats expressing enhanced green fluorescent protein (GFP) in VP MNCs (Figures 2A–2D) and by intracellular recordings from the VP-rich zone of the supraoptic nucleus MNCs in
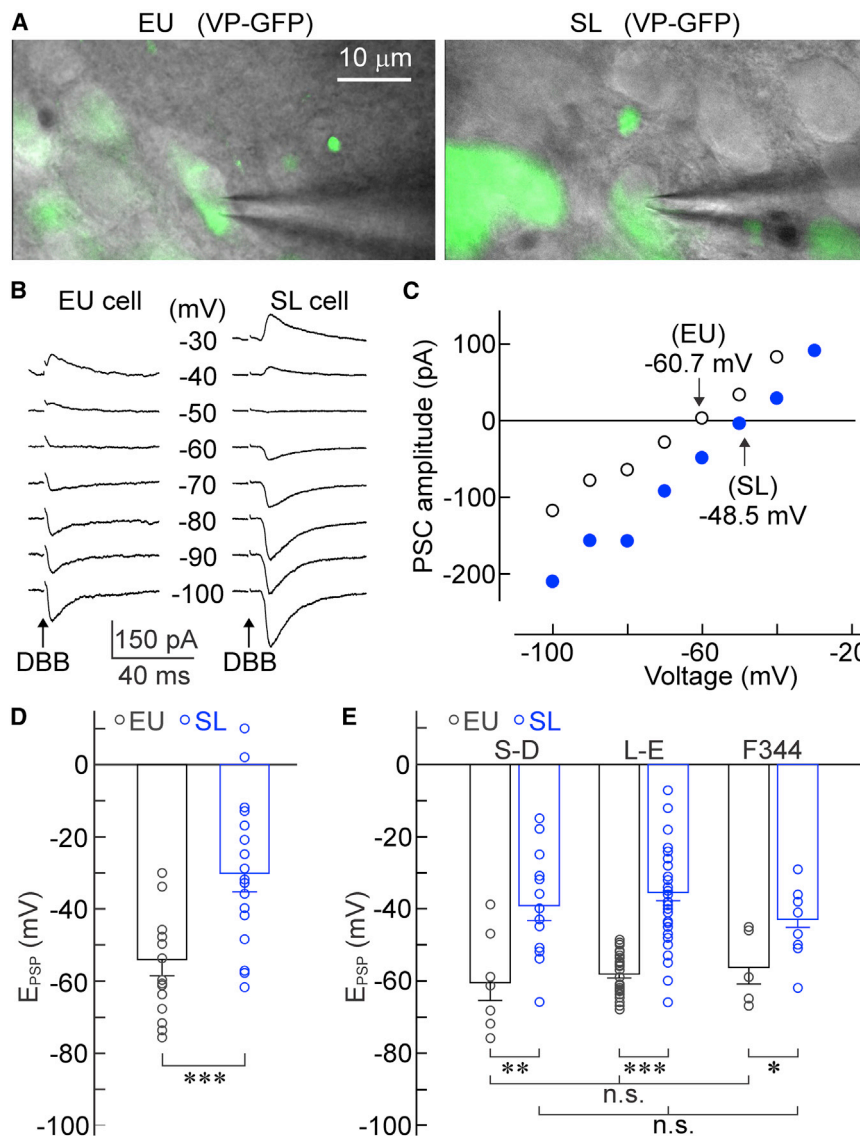
Figure 2. SL Depolarizes E_{GABA} in MNCs from Different Rat Strains

(A) Perforated patch-clamp recordings were made from GFP-expressing VP MNCs in acute hypothalamic slices.

(B) Recordings (average of three sweeps) from the cells in (A) show that electrical stimulation of the DBB (arrow) evokes PSCs, which reverse at different voltages (as indicated) in slices from EU and SL rats.

(C) Amplitude of evoked PSC plotted against membrane voltage for the cells in (A) and (B).

(D) Bar graphs show mean (± SEM) values of E_{GABA} in identified VP MNCs in EU (n = 16, nine rats) and SL (n = 19, six rats) slices. Circles superimposed on the bars plot values determined in all cells tested in both conditions.

(E) Bar graphs show mean (± SEM) values of E_{GABA} (circles show individual values) determined by intracellular recording of MNCs in Sprague-Dawley (S-D), Long Evans (L-E), and Fischer 344 (F344) EU rats (n = 7, four rats; 27, 13 rats; 5, three rats, respectively) or SL rats (n = 13, two rats; 33, 11 rats; 14, three rats, respectively). *p < 0.05; ***p < 0.001; n.s. denotes difference not statistically significant.

inhibitory tone that prevails under normal conditions into an excitatory tone in the SL condition.

SL Depolarizes E_{GABA} via Downregulation of KCC2

The depolarizing shift in E_{GABA} observed in SL MNCs indicates that the intracellular concentration of chloride ($[Cl^-]_i$) is increased under these conditions. Because $[Cl^-]_i$ is determined by the relative activity of the Cl^- exporter KCC2 and the Cl^- importer NKCC1 (Chamma et al., 2012), an increase in $[Cl^-]_i$ could be mediated by either an increase in

hypothalamic explants prepared from three different strains of rats (Long Evans, L-E; Sprague-Dawley, S-D; and Fischer 344 rats; Figure 2E).

To establish if differences in E_{GABA} observed in MNCs from EU and SL rats have a functional impact on GABA$_A$R-mediated inhibitory tone, we examined the effects of antagonizing GABA$_A$Rs on spontaneous AP firing rate measured using non-invasive extracellular single-unit recordings. As shown in Figures 3A and 3B, bath application of 10 μM bicuculline caused a significant excitation of MNCs in EU explants (basal 1.9 ± 0.6 Hz versus bicuculline 2.6 ± 0.7 Hz; n = 10; p = 0.0032), consistent with the existence of a significant inhibitory tone under control conditions. Conversely, bath-application of bicuculline significantly inhibited the firing rate of MNCs in SL explants (basal 2.7 ± 0.7 Hz versus bicuculline 0.9 ± 0.4; n = 17; p = 0.0243; both paired t tests). These observations indicate that the depolarizing shift in E_{GABA} induced by SL is sufficient to convert the

NKCC1 activity and/or a decrease in KCC2 activity. To clarify the mechanism mediating the depolarizing shift in E_{GABA} observed in SL MNCs, we examined the functional contribution of these transporters under EU and SL conditions in L-E rats.

Application of the NKCC1 antagonist bumetanide (10 μM) caused a small but significant hyperpolarization of the average value of E_{GABA} in MNCs from EU rats (−4.4 ± 1.9 mV; n = 10; p = 0.047; Figures 4A and 4B). This observation indicates that NKCC1-mediated Cl^- import plays a role in setting the E_{GABA} of MNCs in these rats. If an increase in NKCC1-mediated import was responsible for the positive shift in E_{GABA} caused by SL, we would expect that the hyperpolarizing effect of bumetanide on E_{GABA} would be enhanced in this condition. However, as illustrated in Figures 4A and 4B, application of bumetanide only had a small and non-significant effect on E_{GABA} in SL MNCs (−2.3 ± 2.9 mV; n = 12; p = 0.45). Therefore the effect of SL on E_{GABA} is not mediated by a change in the activity of NKCC1.
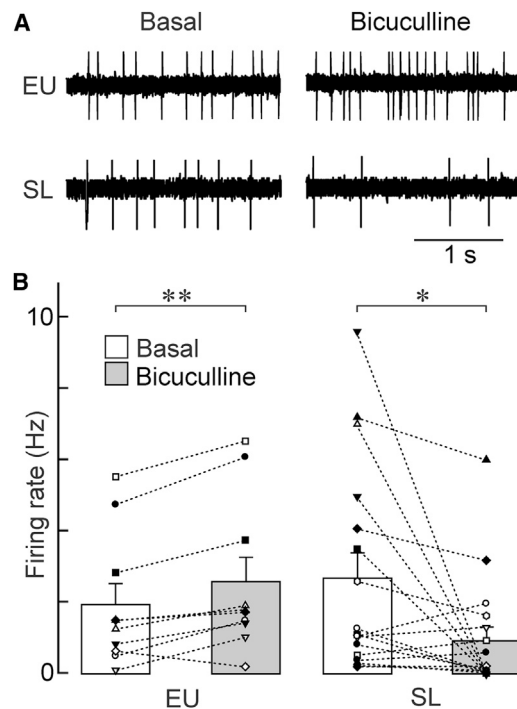
Figure 3. SL Eliminates Inhibitory Tone in Rat MNCs
(A) Excerpts of single-unit activity recorded from MNCs in EU and SL rats before (basal) and during bath applications of 10 μM bicuculline.
(B) Scatter plot displays absolute firing rates of individual MNCs with and without bicuculline (connected by lines) under EU (n = 10, two rats) and SL (n = 17, three rats) conditions. Bar graph overlays represent mean values (± SEM; *p < 0.05; **p < 0.01).

Application of the KCC2 antagonist furosemide (100 μM) caused a significant and reversible depolarization of E_{GABA} in MNCs of EU rats (+9.5 ± 0.8 mV; n = 6; p < 0.001; Figures 4C and 4D), indicating that chloride extrusion contributes to the maintenance of a negative E_{GABA} in MNCs from EU rats. If a decrease in KCC2-mediated Cl^- export was responsible for the depolarization of E_{GABA} in SL MNCs, we would expect that the effect of furosemide would be attenuated in this condition. Indeed, furosemide had no effect on the value of E_{GABA} in MNCs from SL rats (+0.1 ± 0.8 mV; n = 8; p = 0.86; Figures 4C and 4D; paired t test was applied to all bumetanide and furosemide experiments). Taken together, these results indicate that a reduction of KCC2 activity specifically mediates the depolarizing effect of SL on E_{GABA} in MNCs.

To determine if the reduced KCC2 activity caused by SL is associated with a decrease in transporter expression, we performed western blot analysis on lysates of microdissected supraoptic nuclei obtained from EU and SL L-E rats. As shown in Figures 4E and 4F, the average expression of KCC2 was significantly reduced in the supraoptic nucleus of SL rats compared to EU (p = 0.002). Furthermore, immunohistochemical staining revealed a strong expression of KCC2 along the perimeter of VP MNCs in EU rats, and this staining was dramatically lower in SL rats (Figure S3). In agreement with our observations on the effect of bumetanide on E_{GABA}, we observed a small but non-significant decrease in NKCC1 expression. Therefore the depolarization of E_{GABA} caused by SL in MNCs is due specifically to a reduction in Cl^- extrusion mediated by a decrease in KCC2 expression and activity.

SL Causes Activation of TrkB Receptors in the Supraoptic Nucleus

Previous work has shown that a decrease in the expression and functional activity of KCC2 can be mediated by the activation of TrkB upon phosphorylation at tyrosine residue 515 (Y515) (Rivera et al., 2004). We therefore examined if this mechanism was involved in the effect of SL on E_{GABA} in MNCs. We first performed western blot analysis on supraoptic nucleus lysates using antibodies directed against TrkB phosphorylated at Y515 TrkB (p-TrkB) or an unrelated TrkB epitope to measure total TrkB protein (tot-TrkB). As shown in Figures 5A and 5B, the average staining intensity of the p-TrkB protein band was significantly higher in lysates obtained from SL rats than EU rats, when normalized to either a loading control (p-TrkB/GADPH; p = 0.004) or tot-TrkB (p = 0.026; n = 7 for both). These observations indicate that SL causes an increase in TrkB receptor activation without affecting the total amount of TrkB expressed in the supraoptic nucleus.

To determine if TrkB activation is required to mediate the reduction in Cl^- gradient induced by SL, we examined the effect of locally scavenging endogenously released TrkB agonist molecules during the SL treatment. To this end, micro-catheters coupled to osmotic minipumps delivering either TrkB receptor body (TrkB-Fc) or vehicle were stereotaxically implanted unilaterally into the supraoptic nucleus. Delivery of TrkB-Fc using this approach caused a significant reduction in the density of p-TrkB-positive cells observed in the supraoptic nucleus of SL rats compared to the contralateral side (Figure S4), confirming that this approach reduces the extent of TrkB activation caused by SL.

To determine if TrkB activation is required to mediate the effect of SL on E_{GABA}, we examined the effect of reducing TrkB activation by scavenging TrkB agonist molecules with TrkB-Fc during the SL treatment. As shown in Figure 5C, recordings from MNCs in explants prepared from SL rats in which the supraoptic nucleus was infused with vehicle showed an average value of E_{GABA} (−38.8 ± 4.06 mV; n = 13) that was equivalent to that in non-cannulated SL rats (−33.9 ± 2.2 mV; n = 52; p = 0.246) and significantly more depolarized than control (EU) rats (−57.4 ± 1.4 mV; n = 43; p < 0.001). However, the average value of E_{GABA} measured in MNCs recorded from SL rats receiving TrkB-Fc into the supraoptic nucleus (SL-TrkB-Fc rats; −53.2 ± 3.0 mV; n = 21) was significantly more hyperpolarized than vehicle-treated animals (p = 0.003) and equivalent to that observed in EU rats (p = 0.251; all comparisons made using one-way ANOVA followed by Student-Newman-Keuls post-hoc test). Furthermore, as illustrated in Figure 5D, DBB stimulation failed to significantly excite MNCs from SL-TrkB-Fc rats (evoked/baseline AP frequency = 1.63 ± 0.46; n = 6; p = 0.394), whereas the same stimulation induced a robust excitation of MNCs from SL controls (3.37 ± 0.78; n = 16; p < 0.001; both Mann-Whitney rank-sum tests; Figure S5). These observations indicate that TrkB activation is required to mediate the depolarization of E_{GABA} induced by SL in MNCs.

CellPress
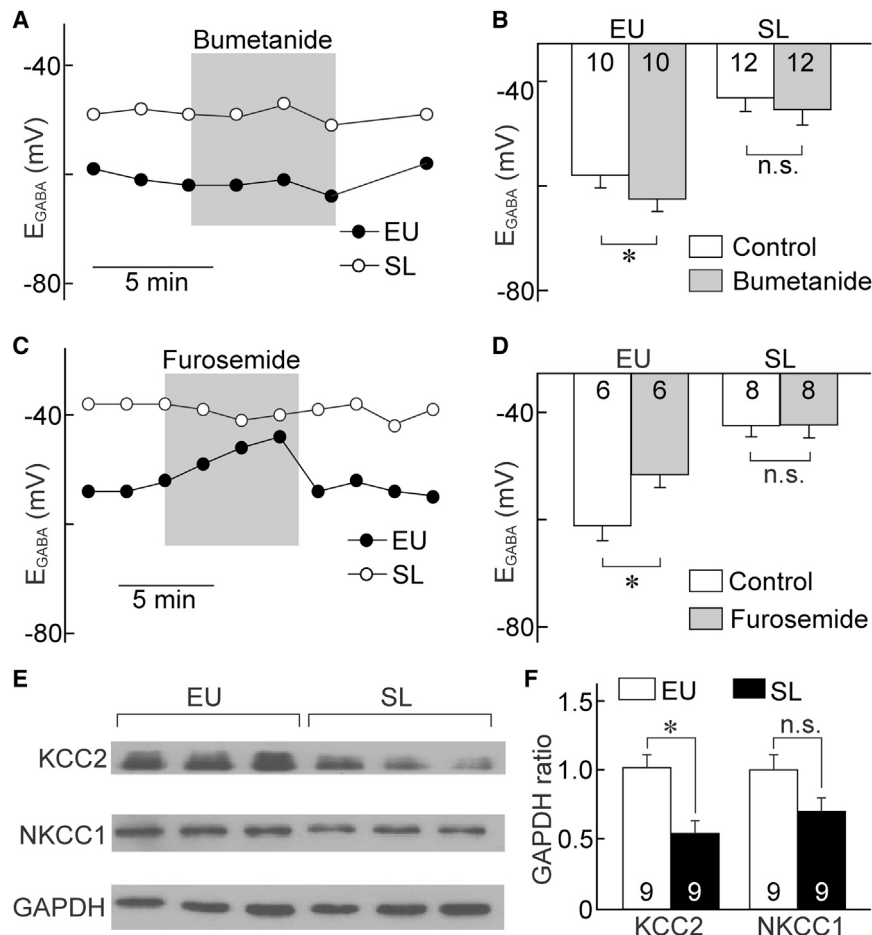
Figure 4. SL Depolarizes E_{GABA} via Downregulation of KCC2

(A) A representative time plot of E_{GABA} measured from EU and SL MNCs before, during, and after application of bumetanide (shaded area).

(B) Bar graphs compare mean values (± SEM) of E_{GABA} measured with and without bumetanide in groups of MNCs from EU and SL rats (n shown on bars; four and six rats, respectively).

(C and D) Same as (A) and (B) but with application of furosemide (three rats in each group).

(E) Sample western blot showing reduced staining for KCC2 (~175 kDa), but not for NKCC1 (~130 kDa) nor loading control (GAPDH; ~38 kDa) in lysates of supraoptic nucleus obtained from EU and SL rats (see also Figure S3).

(F) Bar graphs quantify changes in KCC2 and NKCC1 proteins (normalized to GAPDH) analyzed by western blots (n shown on bars; *p < 0.05; n.s. indicates difference not statistically significant).

## BDNF Is Required for SL-Mediated Cl⁻ Gradient Collapse in MNCs

The activation of TrkB receptors can be mediated by ligands including brain-derived neurotrophic factor (BDNF), neurotrophin 4/5 (NT 4/5), and NT 3 (Boulle et al., 2012). However, previous work has shown that BDNF transcription is increased during physiological and pathological states under which Cl⁻ gradient collapse is evident in neurons (Gall, 1993; Rivera et al., 2002), and that the transcription and secretion of BDNF by VP MNCs increases during hyperosmotic stress (Arancibia et al., 2007). To determine if BDNF is required for SL-mediated collapse of the Cl⁻ gradient in MNCs, we examined the effect of knocking down the level of BDNF in vivo using a short-hairpin RNA (shRNA) that selectively inhibits BDNF synthesis (BDNF-shRNA; Figure S6).

Adeno-associated viruses (AAV) driving production of BDNF-shRNA or a scrambled sequence (scr-shRNA; used as control) were first administered by intracerebroventricular (i.c.v.) injection in anesthetized rats, and the animals were allowed to recover for 4–6 weeks prior to tissue collection for western blot analysis. As illustrated in Figures 6A and 6B, the average expression of BDNF in the anterior hypothalamus of BDNF-shRNA-treated rats was significantly lower than controls (−33.5 ± 19.3% relative to controls; n = four rats in each group; p = 0.044). We next examined

the effects of delivering these AAVs by direct stereotaxic injection into the supraoptic nucleus. This procedure significantly reduced the average staining intensity of immunohistochemically detected BDNF in the supraoptic nucleus of rats having received BDNF-shRNA (60.1% ± 13.7%; n = 3 rats; p = 0.037) compared to scr-shRNA (100.0% ± 7.1%; n = four rats; Figure S7).

To determine if the TrkB-dependent collapse of Cl⁻ gradient and inhibitory signaling induced by SL is mediated by BDNF, we examined the effects of DBB stimulation on MNCs in hypothalamic explants from SL rats having normal and reduced expression of BDNF within the supraoptic nucleus. As found in otherwise intact SL rats, MNCs recorded from the supraoptic nucleus of SL rats having received scr-shRNA were commonly depolarized and excited by DBB-mediated activation of GABA$_A$Rs (Figure 6C) at voltages near threshold. In contrast, MNCs recorded from SL rats having received BDNF-shRNA displayed hyperpolarizing and inhibitory responses to DBB stimulation (Figure 6C). Moreover, the value of E_{GABA} measured in MNCs from SL rats subjected to BDNF knockdown (−56.2 ± 5.4 mV; n = 10) was significantly more hyperpolarized than in scr-shRNA animals (−38.3 ± 2.6 mV; n = 9; p = 0.005; one-way ANOVA and Student-Newman-Keuls posthoc test; Figure 6D) and was equivalent to EU controls (p = 0.806; Figure 6D). These results indicate that BDNF is the endogenous TrkB agonist responsible for the collapse in Cl⁻ gradient observed in SL rats.

Activated Microglia Are Not Required for Cl⁻ Gradient Collapse

Previous studies have shown that BDNF can be released either by activated microglia (Coull et al., 2005) or by neuronal somata and dendrites (Kolarow et al., 2007; Kuczewski et al., 2009). A previous study has reported that microglia in the supraoptic

CellPress

A
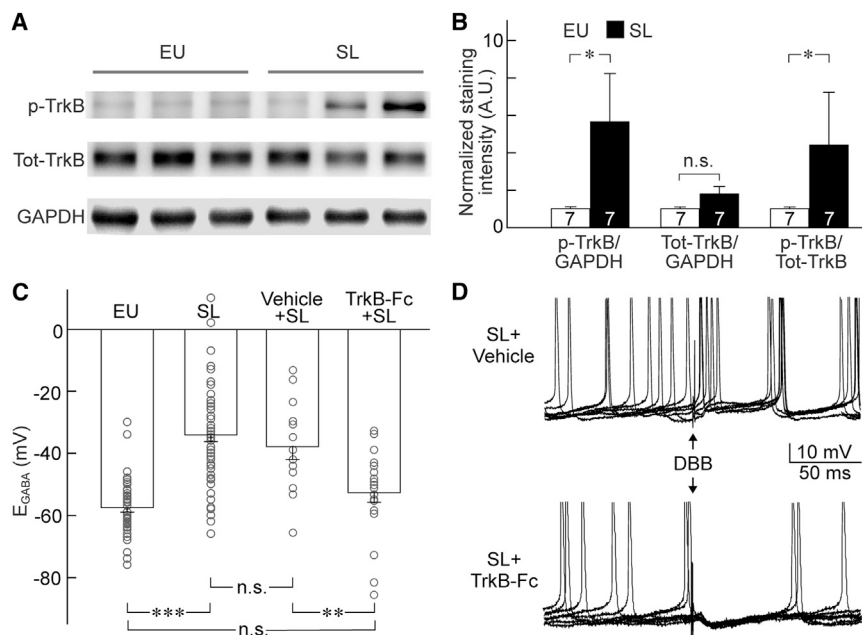
Figure 5. TrkB Receptor Activation Mediates E_{GABA} Shift in SL Rats

(A) Representative western blot showing Y515-phosphorylated TrkB (p-TrkB), total TrkB (tot-TrkB) (both at ~85 kDa), and loading control (GAPDH; ~38 kDa) in supraoptic nucleus lysates from EU and SL rats (see also Figure S4).

(B) Bar graphs show relative staining intensities of p-TrkB and tot-TrkB normalized to GAPDH or tot-TrkB.

(C) Summary of E_{GABA} measurements in MNCs in un-instrumented EU and SL rats, together with values from MNCs recorded from explants prepared from SL rats having received vehicle or TrkB-Fc into the ipsilateral supraoptic nucleus during SL treatment. Scatter plots with bar overlay display individual and mean (± SEM) values of E_{GABA} obtained from EU (n = 43, 22 rats), SL (n = 52, 17 rats, all strains), Vehicle + SL (n = 13, two rats), and TrkB-Fc + SL (n = 21, four rats). *p < 0.05; **p < 0.01; ***p < 0.001; n.s. indicates difference not statistically significant.

(D) Panels show the effects of DBB stimulation (arrows) on membrane voltage measured by intracellular recording from MNCs in explants prepared from vehicle-treated or TrkB-Fc-treated SL rats (six sweeps each). Note the prominent IPSP and inhibition of AP firing observed in the TrkB-Fc-treated cell (see also Figure S5).

nucleus become activated during SL (Ayoub and Salm, 2003). Therefore we investigated the possibility that these cells might provide the BDNF underlying the SL-mediated Cl⁻ gradient collapse. We first examined the morphology of microglia in the supraoptic nucleus using immunohistochemical detection of the microglial marker ionized calcium-binding adaptor molecule 1 (Iba1). In agreement with previous work, we found that microglia in the supraoptic nucleus of EU rats resemble those in resting states and that SL treatment leads to an activation of these cells displayed as a significant hypertrophy of their somata and processes (Figure 7A). Indeed, images of the supraoptic nucleus from SL rats showed a significantly greater Iba1-positive surface area than those from EU rats (p = 0.002 with t test; n = 12 sections from three rats in each group; Figure 7B).

In order to examine whether the activation of microglia is linked with the SL-induced Cl⁻ gradient collapse, we tested the effect of inhibiting microglial activation on the E_{GABA} of MNCs in the supraoptic nucleus. While undergoing the SL treatment, one group of rats concurrently received daily intraperitoneal (i.p.) injections of minocycline hydrochloride (50 mg/kg), a compound that crosses the blood-brain barrier and reduces microglial activation in the brain (Fan et al., 2007). Another group of rats undergoing identical SL treatment received injections of equal amounts of saline as controls. As illustrated in Figure 7C, the mean value of E_{GABA} measured in MNCs from minocycline-treated SL rats (−37.3 ± 4.3 mV; n = 9) remained significantly more depolarized than EU rats (p < 0.001) and was equivalent to saline-injected SL rats (−30.4 ± 5.0 mV; n = 7; p = 0.560) or uninjected SL controls (p = 0.476; all one-way ANOVA followed by Student-Newman-Keuls post-hoc test). These results indicate that microglial activation is not required for SL-mediated collapse of the Cl⁻ gradient in MNCs.

SL Impairs BR-Mediated Inhibition of MNCs

To extend the functional significance of the findings reported above, we next determined if the loss of GABA$_A$R-mediated inhibition caused by SL observed during in vitro recordings was sufficient to impair the BR-mediated inhibition of VP MNCs in vivo. Since it is well established that intravenous (i.v.) injection of α-adrenoreceptor agonists such as phenylephrine (PE) inhibits firing in VP MNCs via BR activation (Cunningham et al., 2004; Renaud and Bourque, 1991; Renaud et al., 1988), we examined whether this response is diminished in SL rats. In single-unit extracellular recordings from VP MNCs in urethane-anaesthetized rats, i.v. infusion of PE (2.5 μg/kg) raised the mean arterial pressure by an equivalent amount in EU (+49.8 ± 5.3 mmHg, n = 14) and SL animals (+53.9 ± 5.9 mmHg, n = 16; p = 0.61). However, the significant inhibition of firing observed in neurons recorded in EU rats (−40.0 ± 10.1%; n = 10; p = 0.004; Wilcoxon signed-rank test) was eliminated in SL rats (−4.5 ± 26.6%; n = 17; p = 0.0784; paired t test; Figures 8A and 8B). Moreover, unlike in EU rats where VP MNCs were either inhibited (9/10 cells) or unaffected (1/10 cells), a significant proportion of VP MNCs in SL rats were excited by BR activation (6/17 cells; p = 0.033; χ^2 test).

Peripheral VP Receptors Contribute to Elevated BP in SL Rats

The results described above indicate that BR inhibition is abolished in VP MNCs after SL. To determine if SL also causes an increase in the basal electrical activity of VP MNCs in vivo, we compared the spontaneous AP firing rate of these cells in EU and SL rats. Average firing rate of VP MNCs in SL rats was significantly higher (9.4 ± 1.2 Hz, n = 23) than that in EU rats (5.5 ± 0.8 Hz, n = 13; p < 0.05; data not shown), consistent with the increased VP secretion observed after SL (Ludwig et al., 1996).
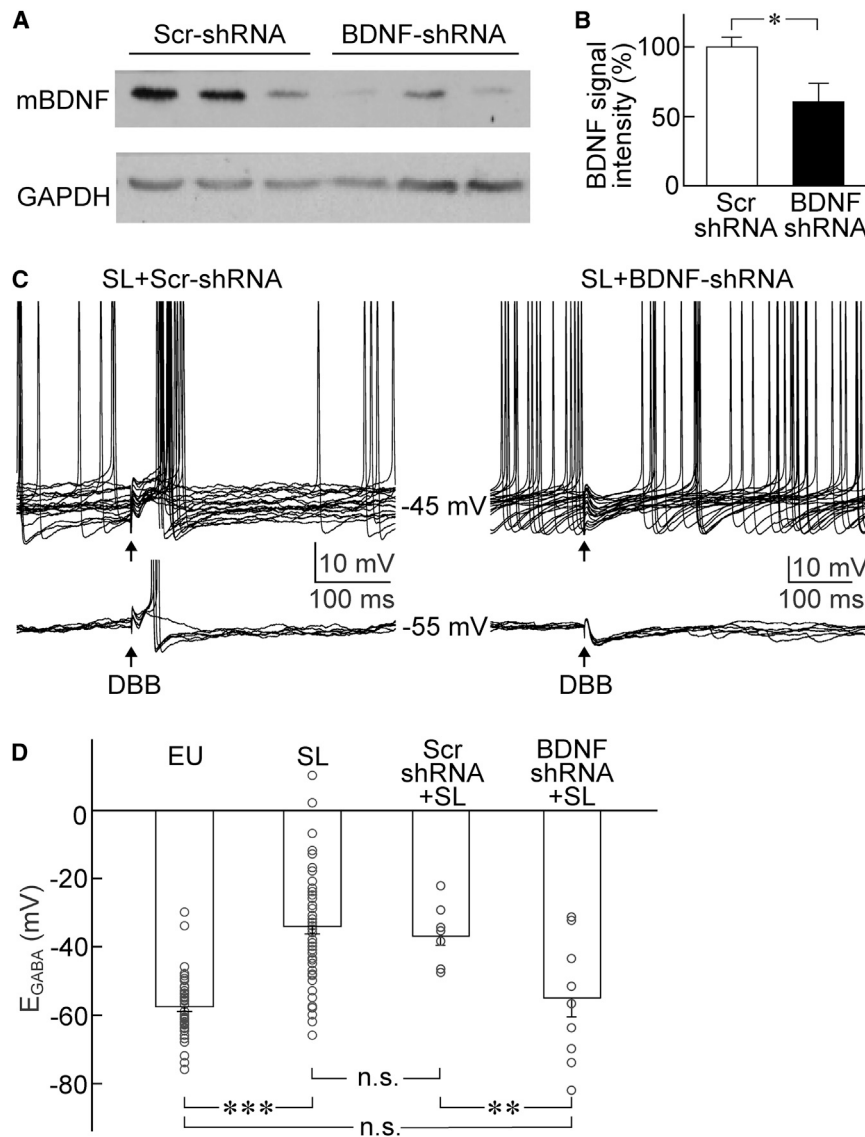
Figure 6. AAV-Mediated Knockdown of BDNF Prevents SL-Induced E_{GABA} Shift

(A) Representative western blot shows that in vivo delivery of BDNF-shRNA via i.c.v. injection of recombinant AAV reduces the expression of mature BDNF (mBDNF,∼14 kDa) in the anterior hypothalamus compared to the scrambled (Scr)-shRNA control. GAPDH (∼38 kDa) was used as loading control (see also Figure S6).

(B) BDNF immunostaining in the supraoptic nucleus of SL rats that received stereotaxic infusions of AAVs carrying either BDNF-shRNA (n = 3) or Scr-shRNA (n = 4; see Figure S7). Bars represent mean (± SEM).

(C) Superimposed traces show the effect of DBB stimulation (arrows) on membrane voltage recorded by perforated patch recordings in hypothalamic slices prepared from SL rats having received Scr-shRNA or BDNF-shRNA in the ipsilateral supraoptic nucleus during the SL treatment. Sweeps show the effects of DBB stimulation with baseline voltage set near rheobase (−45 mV; upper; 20 sweeps each) or at −55 mV (i.e., below AP threshold; six sweeps each). Note the prominent IPSP and inhibition of AP firing observed in the BDNF-shRNA-treated cell.

(D) Summary of E_{GABA} measurements in MNCs in un-instrumented EU and SL rats, together with values from MNCs recorded from slices prepared from SL rats having received scr-shRNA or BDNF-shRNA into the ipsilateral supraoptic nucleus during SL treatment. Scatter plots with bar overlay display individual and mean (± SEM) values of E_{GABA} obtained from EU (n = 43, 22 rats), SL (n = 52, 17 rats), Scr-shRNA+SL (n = 9, four rats), and BDNF-shRNA+SL rats (n = 10, 6 rats). *p < 0.05; **p < 0.01; ***p < 0.001; n.s., not statistically significant.

To determine if an increase in firing and secretion by VP MNCs plays a role in the regulation of BP during SL, mean arterial pressure (MAP) was monitored by radio telemetry in freely moving rats. As illustrated in Figure 8C, MAP rose steadily during the course of the 7 day SL treatment (basal BP: 97.7 ± 1.9 mmHg; day 7: 113.5 ± 2.1 mmHg; n = 10; p < 0.001), whereas MAP remained stable in EU rats over the same time period (basal BP: 98.3 ± 2.5 mmHg; day 7: 100.6 ± 2.2 mmHg; n = 6; p = 0.473; one-way repeated-measures ANOVA with Student-Newman-Keuls post-hoc test). To determine if peripheral VP receptors contribute to the increase in BP induced by SL, we examined the effect of SL on MAP in rats receiving a continuous systemic infusion of dGly[Phaa1,d-tyr(et), Lys, Arg]VP, a VP receptor type 1 (V1R) antagonist. As shown in Figure 8C, the SL-mediated increase in MAP was significantly lower in rats treated with the V1R antagonist (Δ day 7; +8.8 ± 2.5 mmHg; n = 6) when compared to SL controls (+15.1 ± 1.0 mmHg; n = 10; p = 0.03).

DISCUSSION

GABA Hyperpolarizes and Inhibits MNCs in EU Rats

Previous extracellular recordings in vivo have shown that local application of GABA inhibits the electrical activity of MNCs in the rat supraoptic nucleus (Arnauld et al., 1983) and that inhibition of VP MNCs due to BR activation requires local GABA$_A$Rs (Jhamandas and Renaud, 1986). In agreement with these observations, a previous study reported that the value of E_{GABA} measured by perforated patch recording in VP MNCs in vitro lies below the threshold for action potential discharge (Kim et al., 2013). However, this result is contradicted by another study reporting that E_{GABA} is depolarized in VP MNCs and that GABA excites these neurons in hypothalamic slices under control conditions (Haam et al., 2012). Because this is a critical issue for our understanding of the network basis for regulation of MNCs, we re-examined this issue using a variety of approaches.
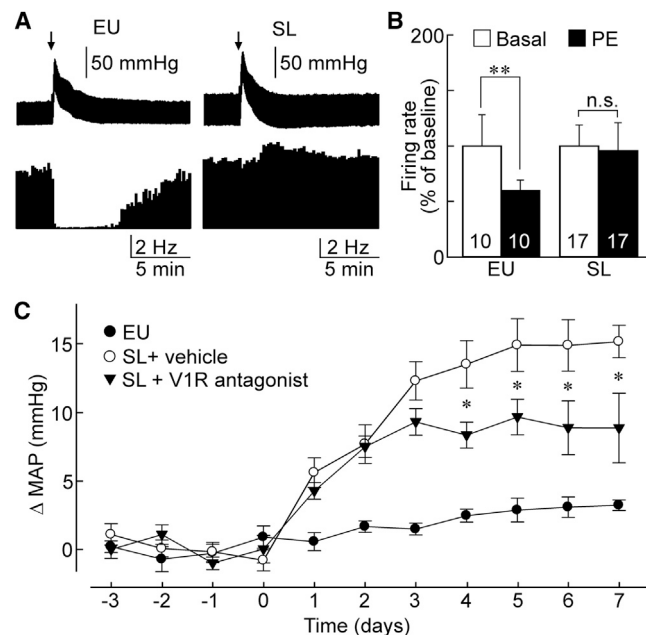
CellPress
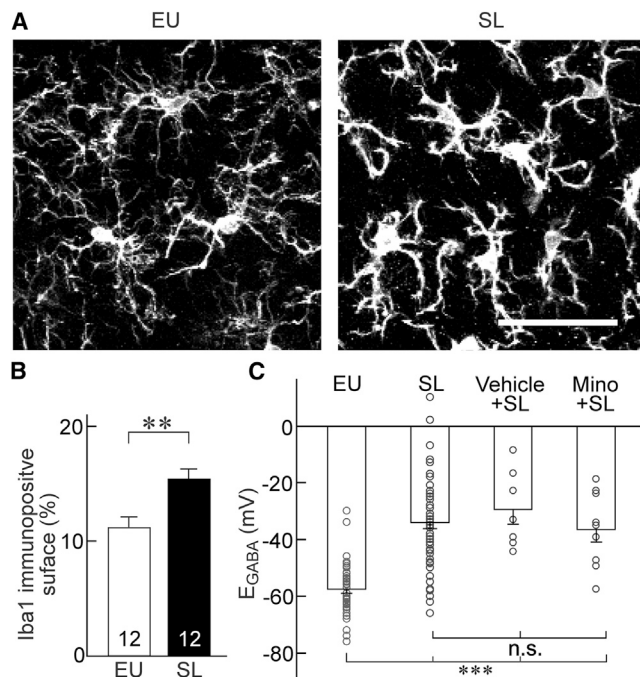
Figure 7. SL-Induced Microglial Activation Does Not Mediate SL Effect on E_{GABA}

(A) Confocal images show SL-induced activation of microglia in the supraoptic nucleus, visualized by Iba1 immunohistochemistry (scale bar = 20 μm).

(B) Bar graphs show the mean (± SEM) percentage of Iba1 immunopositive surface area in images of supraoptic nucleus from SL rats (n = 12, three rats) and EU rats (n = 12, three rats).

(C) Scatter plots with bar overlay display individual and mean (± SEM) values of E_{GABA} obtained from EU (n = 43, 22 rats) and SL rats (n = 52, 17 rats), together with those from SL rats having received i.p. injections of vehicle (n = 7, three rats) or minocycline (Mino; n = 9, four rats). **p < 0.01; ***p < 0.001; n.s., not statistically significant.

Figure 8. Chronic SL Impairs BR Inhibition of VP MNCs and Increases BP

(A) Extracellular single-unit recordings of AP firing rate in VP MNCs (lower) and arterial pressure (upper) from EU and SL rats in vivo. PE was injected (i.v.) at the arrows to increase arterial pressure.

(B) Bar graphs plot mean (± SEM) percent changes in firing rate (relative to baseline) induced by PE in groups of MNCs from EU and SL rats (**p < 0.01; n.s., not statistically significant).

(C) Measurements of changes in mean arterial pressure (ΔMAP) observed during the course of SL (starting day 1) using radio telemetry, in EU rats (n = 6 rats), or SL rats receiving continuous i.p. infusions of either vehicle (n = 10 rats) or V1R antagonist (n = 6 rats; *p < 0.05; n.s., not statistically significant).

As shown in Figure 2, gramicidin-based perforated patch recordings from identified VP MNCs in the supraoptic nucleus of hypothalamic slices showed that E_{GABA} is consistently and significantly more hyperpolarized than rheobase (−45 mV) in EU rats. Identical results were obtained during intracellular recordings from the VP-rich (ventral-caudal) zone of the supraoptic nucleus in hypothalamic explants prepared from three different strains of rats (Figure 2E). Our findings are therefore in agreement with previous studies indicating that MNCs in EU rats maintain a hyperpolarized E_{GABA} that allows these cells to be potently inhibited by GABAergic synaptic inputs, including those activated by BR activation. Although we have no explanation for the discordant results reported by Haam and colleagues, the present work and studies by others have shown that the neuronal Cl$^-$ gradient is a labile parameter that can be rapidly collapsed as a result of stress (Hewitt et al., 2009) or experimental procedures (Dzhala et al., 2012).

Reduced KCC2 Expression Depolarizes E_{GABA} during SL

A previous study has reported that the depolarizing shift in E_{GABA} observed in MNCs from SL S-D rats is caused by an increase in the activity and expression of the Cl$^-$ importer NKCC1 (Kim et al.,

2011). Although our experiments and those of Kim and colleagues revealed an equivalent SL-induced shift in E_{GABA}, our electrophysiological analysis with blockers of KCC2 and NKCC1 indicated that this effect is due to a SL-mediated reduction in KCC2 activity, rather than an increase in NKCC1 activity. Our findings were corroborated by western blot analysis showing that KCC2 expression is significantly reduced by SL in L-E rats, whereas NKCC1 levels are not significantly increased (Figure 4E). The absence of increased NKCC1-mediated Cl$^-$ import in SL rats may seem surprising since [Cl$^-$]$_i$ levels are increased in this condition. However it remains possible that a small residual NKCC1-mediated import could be sufficient to raise [Cl$^-$]$_i$ under conditions where KCC2 activity is depressed. Alternately, the increased value of [Cl$^-$]$_i$ that prevails in MNCs from SL rats could simply result from the cumulative effect of Cl$^-$ influx mediated by basal synaptic and extrasynaptic GABA$_A$R activity and weakened Cl$^-$ extrusion due to downregulated KCC2. The basis for differences between our results and those of Kim (Kim et al., 2011) are unknown, but two possible explanations should be considered.

First, previous work has shown that the pattern of gene expression is different in the supraoptic nucleus of different rat strains (Hindmarch et al., 2007). Although SL has been found

to cause a depolarization of E_{GABA} in all strains examined so far (Fischer 344, L-E, S-D, and Wistar), it is possible that Cl^- transport is mediated more strongly by NKCC1 in S-D rats and more strongly by KCC2 in L-E rats. Second, the tissue preparation methods used in the two studies were slightly different. Notably, whereas our samples were collected by rapid microdissection of the supraoptic nucleus immediately following removal of the brain, samples obtained by Kim and colleagues were collected by excision of the supraoptic nucleus from hypothalamic slices. Given the labile nature of KCC2 expression in slices (Dzhala et al., 2012), it is possible that this procedure can mask the true contribution of KCC2 to Cl^- homeostasis in the supraoptic nucleus. Given the ubiquitous involvement of changes in KCC2 expression as a mediator of altered $[Cl^-]_i$ in various pathophysiological states, and the lesser degree of trauma applied to the tissue used in our western blot and electrophysiological analysis (i.e., acute explants), we believe that KCC2 serves as the predominant regulator of $[Cl^-]_i$ in the supraoptic nucleus and that its modulation is a key contributor to the depolarizing shift in E_{GABA} induced by SL in vivo.

BDNF-Activated TrkB Depolarizes E_{GABA} during SL

Our results show that SL causes the functional activation of TrkB receptors in MNCs of the supraoptic nucleus and that activation of these receptors is required to mediate the depolarization of E_{GABA} in response to this stimulus. Previous studies have shown that KCC2 activity can be regulated by several types of TrkB-dependent mechanisms. For example, TrkB activation has been shown to suppress KCC2 transcription through a cAMP response element-binding protein (CREB)-dependent pathway (Rivera et al., 2004). Our observation that KCC2 protein expression is significantly reduced in SL rats is consistent with this mechanism and suggests that a decrease in KCC2 synthesis may contribute significantly to the decrease in KCC2 activity associated with this condition. However, the involvement of post-translational mechanisms cannot be excluded. For example, TrkB activation has been shown to activate calpain (Zadran et al., 2010), which can reduce KCC2 activity by proteolytic cleavage (Puskarjov et al., 2012). Moreover, TrkB activation can increase NMDA receptor activity by phosphorylation (Carreño et al., 2011), and Ca^{2+} influx through NMDA receptors has been shown to reduce KCC2 activity via endocytosis (Lee et al., 2011). The specific mechanism(s) by which TrkB activation downregulates KCC2 in SL MNCs remain to be determined.

Our shRNA-mediated knockdown experiments revealed that BDNF is the agonist responsible for the activation of TrkB in response to SL in MNCs. BDNF has also been identified as a mediator of altered neuronal Cl^- homeostasis in neuropathic pain (Coull et al., 2005) and morphine hyperalgesia (Ferrini et al., 2013). In the latter models, experiments revealed that activated microglia secrete the BDNF required for TrkB activation and downregulation of KCC2 (Ferrini and De Koninck, 2013). Although SL causes microglial activation in the rat supraoptic nucleus (Figure 7) (Ayoub and Salm, 2003), the effect of SL on E_{GABA} in MNCs was not prevented by inhibiting microglial activation in vivo. Therefore, an alternate possibility is that BDNF is released by the MNCs themselves. Indeed, BDNF is known to be released by many types of neurons in an activity-dependent

manner (Kuczewski et al., 2009), and previous work has shown that BDNF is synthesized by MNCs (Carreño et al., 2011). Moreover, acute hyperosmotic conditions, which excite MNCs (Bourque, 2008), have been shown to enhance the transcription of BDNF by MNC somata and to stimulate BDNF release by the dendrites of these neurons in the supraoptic nucleus in vivo (Aliaga et al., 2002; Arancibia et al., 2007). Therefore SL is likely to trigger the activation of TrkB receptors as an autocrine or paracrine response to BDNF release by the MNCs themselves.

High Salt Intake Promotes a VP-Dependent Increase in BP

Increases in plasma sodium associated with a high level of dietary salt intake are linked to elevated BP in salt-sensitive hypertensive patients (He et al., 2013; He and Macgregor, 2012; Schmidlin et al., 2007), but the mechanisms underlying this effect are unclear. Hyperosmolality is a necessary consequence of hypernatremia and thus activates central osmoreceptors (Bourque, 2008). Moreover, the recruitment of central osmoreceptor pathways has been shown to enhance sympathetic tone through an excitation of preautonomic neurons (Toney and Stocker, 2010) and VP release through glutamatergic excitation of MNCs (Trudel and Bourque, 2010). Although both factors could potentially contribute to increases in BP, the activation of BR should normally counteract increases in BP by opposing both mechanisms. However, our in vitro and in vivo results strongly indicate that collapse of the Cl^- gradient eliminates BR inhibition of VP-MNCs during SL, suggesting that this negative feedback mechanism is impaired under these conditions. Moreover, in a significant proportion of MNCs, the depolarizing response to $GABA_A R$ activation appeared to be sufficient to produce an excitatory response to BR activation. By promoting a further excitation of MNCs, this functional switch in the polarity of BR input would eventually result in enhanced VP secretion and thus amplify the contribution of this hormone to the elevation in BP as SL progresses. Indeed, data shown in Figure 8C indicate that circulating VP mediates a significant proportion of the SL-mediated increase in BP and that V1R-mediated contribution to BP increased as a function of time during the SL protocol.

There are three known mechanisms through which circulating VP can modulate BP. First, increases in systemic VP have been shown to enhance BR reflex-mediated decreases in sympathetic output though a V1R-dependent action in the area postrema (Hasser et al., 1997). Second, VP has been shown to activate V1R expressed at the subfornical organ to reduce BP, possibly via a reduction of sympathetic output (Smith and Ferguson, 1997). However, in both cases V1R activation promotes a lowering of BP. It is therefore unlikely that these mechanisms contribute to the elevated BP found under SL. Third, V1Rs are widely expressed in vascular smooth muscle where they mediate a potent vasoconstrictor effect (Henderson and Byron, 2007). Moreover, VP levels reportedly associated with SL (Ludwig et al., 1996) appear to be sufficient to induce vasoconstriction (Henderson and Byron, 2007), suggesting that increases in circulating VP associated with SL could contribute to the elevation of BP observed under such conditions. This hypothesis is directly supported by our finding that antagonism of V1R partially reversed the SL-mediated elevations in BP. While the nature of

the residual component in SL-induced BP increase after V1 blockade remains undetermined, we suspect a possible role of hyperosmolality-induced increase in sympathetic outflow (Toney and Stocker, 2010).

Concluding Remarks

Our results show that high salt intake can cause a collapse of the Cl^- gradient across VP neurons and abolish BR-mediated negative feedback inhibition of these cells due to the activity-dependent release of BDNF and downregulation of KCC2 that results from the autocrine activation of TrkB receptors. The elevated firing rate of MNCs associated with this condition leads to an increase in VP secretion and a significant V1R-dependent increase in BP. These findings show that state-dependent changes in neurotrophin signaling can mediate pathological consequences by promoting plastic changes in hypothalamic homeostatic networks.

EXPERIMENTAL PROCEDURES

Drugs and Antibodies

Kynurenic acid was purchased from Sigma. DNQX (Tocris) was kept at a stock concentration of 20 mM in dimethyl sulfoxide (DMSO) (Sigma). Bicuculline methochloride, furosemide, bumetanide, and gabazine were obtained from Tocris. V1R antagonist dGly[Phaa1,d-tyr(et), Lys, Arg]VP was purchased from Bachem. TrkB-Fc chimera was purchased from R&D Systems. Antibodies from commercial sources: KCC2 (1:500), pan-TrkB (1:1,000), and GAPDH (1:5,000) from Millipore; BDNF (Santa Cruz Biotechnology; 1:100 for WB, 1:300 for IHC); Y515 phosphorylated TrkB from Abcam (1:100); and Iba1 from Wako chemicals (1:1,000). NKCC1 antibody (1:500) was generously provided by Dr. R. James Turner (NIH). VP-neurophysin antibody (mouse monoclonal, 1:100) was kindly provided by Dr. Hal Gainer (NIH).

Animals

Adult male rats were maintained on a 12:12 hr light cycle and provided with ad libitum access to food and water except where indicated in specific protocols. All procedures involving animals were conducted according to protocols approved by the Facility Animal Care Committee of McGill University, University of Otago Animal Ethics Committee, and the Institutional Animal Care and Use Committee of the UNT Health Science Center.

In Vitro Electrophysiological Recordings

Acute rat hypothalamic explants prepared as previously (Ghamari-Langroudi and Bourque, 2001) were superfused ($\sim$1–1.5 ml/min) with warm (31°C–33°C) oxygenated (95% O_2; 5% CO_2, pH 7.35) artificial cerebrospinal fluid (ACSF) comprising NaCl (104 mM), $NaHCO_3$ (26 mM), NaH_2PO_4 (1.23 mM), KCl (3 mM), $MgCl_2$ (1 mM), $CaCl_2$ (2 mM), and D-glucose (10 mM), and mannitol was added to the desired osmolality. For extracellular recordings, KCl was increased to 4 mM and CaCl was reduced to 1 mM. Recordings were made using micropipettes (extracellular, 15–20 MΩ; intracellular, 80–110 MΩ) filled with 2 M K-acetate.

Acute hypothalamic slices 400 μm thick were cut at an angle of 38° relative to the surface of the cortex as described previously (Trudel and Bourque, 2010) and submerged in warm oxygenated ACSF (same as above). Gramicidin (Sigma) was dissolved in DMSO at a stock concentration of 0.05 mg/μl and diluted 1:500 into K-gluconate-based internal pipette solution. Borosilicate glass patch pipettes (3–6 MΩ) were pulled and filled with the gramicidin-containing internal solution. Recordings from identified VP neurons were made by targeting eGFP-expressing neurons in slices prepared from transgenic VP-eGFP Wistar rats. After establishing gigaohm seals with target cells, E_{GABA} measurements were made after the pipette resistance dropped to values between 40 and 80 MΩ. For both preparations, electrical stimulation was performed using a DS2 Digitimer coupled to a concentric bipolar electrode (FHC, Inc.) placed within the DBB.

In Vivo Electrophysiological Recordings

The pituitary stalk and right SON of urethane-anaesthetized rats (1.25 g/kg, Sigma) were exposed by a ventral approach through the oral cavity. Extracellular single-unit recordings were made using micropipettes (15–40 MΩ) filled with 0.9% saline. MNCs were identified by antidromic spikes elicited from pituitary stalk stimulation with a bipolar electrode (Science Products GmBH). VP-MNCs were characterized by their spontaneous phasic activity or by a lack of excitation following intravenous (i.v.) cholecystokinin (CCK) injection (20 μg/kg, 0.5 ml/kg in 0.9% saline), or as oxytocin-MNCs by transient excitation following CCK injection (Sabatier et al., 2004). At the end of the experiments, the rats were killed by anesthetic overdose (60 mg/kg pentobarbitone or 1 g/kg urethane, i.v.).

SON Tissue Lysate Preparation

Brains of age-matched EU and 7 day SL rats were rapidly removed and submerged into oxygenated isosmotic ACSF, and then SON tissue blocks (1 mm^3) or the entire anterior hypothalami were excised using a pair of angled spring scissors. Tissue lysates were then prepared by trituration in HEPES-based buffer followed by centrifugation. Western blotting experiments were performed using standard procedures and intensities of bands were quantified using ImageJ (NIH).

Immunohistochemistry

Brains of age-matched EU and 7 day SL Long Evans rats perfused with 4% paraformaldehyde (Sigma) were sectioned in the coronal plane (50 μm thick) using a vibratome and stained immunohistochemically using various primary antibodies listed above. Once prepared into slides, images of immunostained structures were captured as continuous stacks of confocal images (1 μm thick) using an Olympus FV1000 scanning laser confocal microscope equipped with a krypton/argon mixed gas laser. All of the analysis was performed with ImageJ (NIH).

Drug Infusion of Unilateral SON

Rats were instrumented with unilateral cannula targeted at the SON as previously described (Carreño et al., 2011). Under isoflurane anesthesia (2%), the rats were placed in a stereotaxic frame (Kopf Instruments), and a 28 gauge cannula (Plastics One) was placed in the right SON. Each cannula was connected to an osmotic pump implanted subcutaneously around the neck region of rats (ALZET) filled with either saline or TrkB-Fc. After 7–10 days of recovery, rats underwent a 7 day SL protocol and then were prepared into hypothalamic explant preparations for in vitro electrophysiological experiments. The efficiency of TrkB-Fc infusion was tested by post-hoc immunohistochemistry.

AAV-Mediated Knockdown of BDNF in the Supraoptic Nucleus

Adeno-associated virus (AAV) serotype 2 conjugated with shRNA directed against BDNF was custom-generated (Vector Biolabs). To test the effectiveness of the shRNA's ability to induce a specific knockdown of BDNF in vitro, HEK293T cells were transfected with 2 μg BDNF with or without BDNF-shRNA. Twenty-four hours later, the conditioned media was collected and concentrated and then run in a western blot. AAV conjugated with either the BDNF- or scrambled (scr)-shRNA (Vector Biolabs) were injected intracerebroventricularly (i.c.v.) into the third ventricle (2 μl) to test the in vivo effectiveness of knockdown in hypothalamic tissue. After 4 weeks the rat brains were harvested and the anterior hypothalami were microdissected and processed for western blotting. To induce a specific knockdown of BDNF in the supraoptic nucleus, rats were stereotaxically injected with AAVs conjugated with either BDNF- or scr-shRNA (1 μl; from Bregma, X: 1.5 mm, Y: −0.5 mm, Z: 7.7 mm). The virus was allowed to express in vivo for 5–6 weeks, after which the rats underwent a 7 day SL treatment. Their brains were harvested and prepared for hypothalamic slices as described above. After patch-clamp recordings, the slices were immersion-fixed in 4% paraformaldehyde overnight and processed for post-hoc immunohistochemistry to confirm the success of knockdown.

Inhibition of Microglial Activation via Intraperitoneal Injections of Minocycline

Minocycline hydrochloride (Sigma) was dissolved in 0.9% saline, and appropriate amounts of NaOH were added to adjust the pH to $\sim$7.4. Each rat

CellPress

received a daily dose of 50 mg/kg i.p. for 7 days, during which they also underwent SL treatment. A control group of rats received injections of equal amounts of saline. On the last day of SL, the rat brains were harvested and made into hypothalamic slice preparations, and patch-clamp recordings were performed.

Radio Telemetry Measurement of BP and In Vivo Infusion of VP Antagonist

As previously described (Cunningham et al., 2012), rats were implanted with an abdominal aortic catheter attached to a TA11PA-C40 radio telemetry transmitter under isoflurane anesthesia (2%). The transmitter was secured to the abdominal muscle and remained in the abdominal cavity for the duration of the experiment. After a 2 week recovery period, MAP signals from the telemetry device were recorded during a 7 day SL protocol using a Dataquest IV radio telemetry system (Data Sciences Inc.). Prior to SL treatment, a subgroup of these rats was also implanted with an osmotic minipump (ALZET) in a subcutaneous pouch made between the scapulae under isoflurane anesthesia (2%) for subcutaneous drug infusion.

Statistics

All values in this study are reported as mean ± the standard error of the mean (SEM). Unless explicitly stated, statistical differences between mean values were tested using Student's two-tailed t test. All statistical tests were performed with Sigmaplot 12.3 (SPSS Inc.) or Prism 5 (Graphpad Software Inc.). Data points above or below twice the standard deviation from the mean were excluded from statistical comparisons. Differences between values were considered to be significant when $p < 0.05$.

SUPPLEMENTAL INFORMATION

Supplemental Information includes Supplemental Experimental Procedures and seven figures and can be found with this article online at http://dx.doi.org/10.1016/j.neuron.2014.12.048.

AUTHOR CONTRIBUTIONS

K.Y.C., D.L.V., C.H.B., J.T.C, P.A.B., and C.W.B. designed experiments. K.Y.C. performed in vitro recordings. S.Y.H. performed in vivo recordings. K.Y.C., D.L.V., and B.S. performed immunohistochemistry. P.G. and B.A.K. performed western blotting. K.Y.C. and D.L.V. performed stereotaxic injections of AAV-shRNA and minocycline injections. J.T.C. performed telemetry measurements of mean arterial pressures. K.Y.C. and C.W.B. cowrote the manuscript.

REFERENCES

Aliaga, E., Arancibia, S., Givalois, L., and Tapia-Arancibia, L. (2002). Osmotic stress increases brain-derived neurotrophic factor messenger RNA expression in the hypothalamic supraoptic nucleus with differential regulation of its transcripts. Relation to arginine-vasopressin content. Neuroscience 112, 841–850.

Arancibia, S., Lecomte, A., Silhol, M., Aliaga, E., and Tapia-Arancibia, L. (2007). In vivo brain-derived neurotrophic factor release and tyrosine kinase B receptor expression in the supraoptic nucleus after osmotic stress stimulus in rats. Neuroscience 146, 864–873.

Arnauld, E., Cirino, M., Layton, B.S., and Renaud, L.P. (1983). Contrasting actions of amino acids, acetylcholine, noradrenaline and leucine enkephalin on the excitability of supraoptic vasopressin-secreting neurons. A microiontophoretic study in the rat. Neuroendocrinology 36, 187–196.

Ayoub, A.E., and Salm, A.K. (2003). Increased morphological diversity of microglia in the activated hypothalamic supraoptic nucleus. J. Neurosci. 23, 7759–7766.

Boulenguez, P., Liabeuf, S., Bos, R., Bras, H., Jean-Xavier, C., Brocard, C., Stil, A., Darbon, P., Cattaert, D., Delpire, E., et al. (2010). Down-regulation of the potassium-chloride cotransporter KCC2 contributes to spasticity after spinal cord injury. Nat. Med. 16, 302–307.

Boulle, F., Kenis, G., Cazorla, M., Hamon, M., Steinbusch, H.W., Lanfumey, L., and van den Hove, D.L. (2012). TrkB inhibition as a therapeutic target for CNS-related disorders. Prog. Neurobiol. 98, 197–206.

Bourque, C.W. (2008). Central mechanisms of osmosensation and systemic osmoregulation. Nat. Rev. Neurosci. 9, 519–531.

Carreño, F.R., Walch, J.D., Dutta, M., Nedungadi, T.P., and Cunningham, J.T. (2011). Brain-derived neurotrophic factor-tyrosine kinase B pathway mediates NMDA receptor NR2B subunit phosphorylation in the supraoptic nuclei following progressive dehydration. J. Neuroendocrinol. 23, 894–905.

Castren, E., Thoenen, H., and Lindholm, D. (1995). Brain-derived neurotrophic factor messenger RNA is expressed in the septum, hypothalamus and in adrenergic brain stem nuclei of adult rat brain and is increased by osmotic stimulation in the paraventricular nucleus. Neuroscience 64, 71–80.

Chamma, I., Chevy, Q., Poncer, J.C., and Lévi, S. (2012). Role of the neuronal K-Cl co-transporter KCC2 in inhibitory and excitatory neurotransmission. Front Cell Neurosci 6, 5.

Coull, J.A., Boudreau, D., Bachand, K., Prescott, S.A., Nault, F., Sík, A., De Koninck, P., and De Koninck, Y. (2003). Trans-synaptic shift in anion gradient in spinal lamina I neurons as a mechanism of neuropathic pain. Nature 424, 938–942.

Coull, J.A., Beggs, S., Boudreau, D., Boivin, D., Tsuda, M., Inoue, K., Gravel, C., Salter, M.W., and De Koninck, Y. (2005). BDNF from microglia causes the shift in neuronal anion gradient underlying neuropathic pain. Nature 438, 1017–1021.

Cunningham, J.T., Bruno, S.B., Grindstaff, R.R., Grindstaff, R.J., Higgs, K.H., Mazzella, D., and Sullivan, M.J. (2002). Cardiovascular regulation of supraoptic vasopressin neurons. Prog. Brain Res. 139, 257–273.

Cunningham, J.T., Penny, M.L., and Murphy, D. (2004). Cardiovascular regulation of supraoptic neurons in the rat: synaptic inputs and cellular signals. Prog. Biophys. Mol. Biol. 84, 183–196.

Cunningham, J.T., Knight, W.D., Mifflin, S.W., and Nestler, E.J. (2012). An Essential role for DeltaFosB in the median preoptic nucleus in the sustained hypertensive effects of chronic intermittent hypoxia. Hypertension 60, 179–187.

Dzhala, V., Valeeva, G., Glykys, J., Khazipov, R., and Staley, K. (2012). Traumatic alterations in GABA signaling disrupt hippocampal network activity in the developing brain. J. Neurosci. 32, 4017–4031.

Fan, R., Xu, F., Previti, M.L., Davis, J., Grande, A.M., Robinson, J.K., and Van Nostrand, W.E. (2007). Minocycline reduces microglial activation and improves behavioral deficits in a transgenic model of cerebral microvascular amyloid. J. Neurosci. 27, 3057–3063.

Ferrini, F., and De Koninck, Y. (2013). Microglia control neuronal network excitability via BDNF signalling. Neural Plast. 2013, 429815, http://dx.doi.org/10.1155/2013/429815.

Ferrini, F., Trang, T., Mattioli, T.A., Laffray, S., Del'Guidice, T., Lorenzo, L.E., Castonguay, A., Doyon, N., Zhang, W., Godin, A.G., et al. (2013). Morphine

hyperalgesia gated through microglia-mediated disruption of neuronal Cl⁻ homeostasis. Nat. Neurosci. 16, 183–192.

Fujiwara, Y., Tanoue, A., Tsujimoto, G., and Koshimizu, T.A. (2012). The roles of V1a vasopressin receptors in blood pressure homeostasis: a review of studies on V1a receptor knockout mice. Clin. Exp. Nephrol. 16, 30–34.

Gall, C.M. (1993). Seizure-induced changes in neurotrophin expression: implications for epilepsy. Exp. Neurol. 124, 150–166.

Ghamari-Langroudi, M., and Bourque, C.W. (2001). Ionic basis of the caesium-induced depolarisation in rat supraoptic nucleus neurones. J. Physiol. 536, 797–808.

Haam, J., Popescu, I.R., Morton, L.A., Halmos, K.C., Teruyama, R., Ueta, Y., and Tasker, J.G. (2012). GABA is excitatory in adult vasopressinergic neuroendocrine cells. J. Neurosci. 32, 572–582.

Hasser, E.M., Bishop, V.S., and Hay, M. (1997). Interactions between vasopressin and baroreflex control of the sympathetic nervous system. Clin. Exp. Pharmacol. Physiol. 24, 102–108.

He, F.J., and Macgregor, G.A. (2012). Salt intake, plasma sodium, and worldwide salt reduction. Ann. Med. 44 (Suppl 1), S127–S137.

He, F.J., Li, J., and Macgregor, G.A. (2013). Effect of longer term modest salt reduction on blood pressure: Cochrane systematic review and meta-analysis of randomised trials. BMJ 346, f1325.

Henderson, K.K., and Byron, K.L. (2007). Vasopressin-induced vasoconstriction: two concentration-dependent signaling pathways. J. Appl. Physiol. 102, 1402–1409.

Hewitt, S.A., Wamsteeker, J.I., Kurz, E.U., and Bains, J.S. (2009). Altered chloride homeostasis removes synaptic inhibitory constraint of the stress axis. Nat. Neurosci. 12, 438–443.

Hindmarch, C., Yao, S., Hesketh, S., Jessop, D., Harbuz, M., Paton, J., and Murphy, D. (2007). The transcriptome of the rat hypothalamic-neurohypophyseal system is highly strain-dependent. J. Neuroendocrinol. 19, 1009–1012.

Huang, Y., Wang, J.J., and Yung, W.H. (2013). Coupling between GABA-A receptor and chloride transporter underlies ionic plasticity in cerebellar Purkinje neurons. Cerebellum 12, 328–330.

Huberfeld, G., Wittner, L., Clemenceau, S., Baulac, M., Kaila, K., Miles, R., and Rivera, C. (2007). Perturbed chloride homeostasis and GABAergic signaling in human temporal lobe epilepsy. J. Neurosci. 27, 9866–9873.

Jhamandas, J.H., and Renaud, L.P. (1986). A gamma-aminobutyric-acid-mediated baroreceptor input to supraoptic vasopressin neurones in the rat. J. Physiol. 381, 595–606.

Kim, J.S., Kim, W.B., Kim, Y.B., Lee, Y., Kim, Y.S., Shen, F.Y., Lee, S.W., Park, D., Choi, H.J., Hur, J., et al. (2011). Chronic hyperosmotic stress converts GABAergic inhibition into excitation in vasopressin and oxytocin neurons in the rat. J. Neurosci. 31, 13312–13322.

Kim, Y.B., Kim, Y.S., Kim, W.B., Shen, F.Y., Lee, S.W., Chung, H.J., Kim, J.S., Han, H.C., Colwell, C.S., and Kim, Y.I. (2013). GABAergic excitation of vasopressin neurons: possible mechanism underlying sodium-dependent hypertension. Circ. Res. 113, 1296–1307.

Kolarow, R., Brigadski, T., and Lessmann, V. (2007). Postsynaptic secretion of BDNF and NT-3 from hippocampal neurons depends on calcium calmodulin kinase II signaling and proceeds via delayed fusion pore opening. J. Neurosci. 27, 10350–10364.

Kuczewski, N., Porcher, C., Lessmann, V., Medina, I., and Gaiarsa, J.L. (2009). Activity-dependent dendritic release of BDNF and biological consequences. Mol. Neurobiol. 39, 37–49.

Lee, H.H., Deeb, T.Z., Walker, J.A., Davies, P.A., and Moss, S.J. (2011). NMDA receptor activity downregulates KCC2 resulting in depolarizing GABAA receptor-mediated currents. Nat. Neurosci. 14, 736–743.

Lu, B. (2003). BDNF and activity-dependent synaptic modulation. Learn. Mem. 10, 86–98.

Ludwig, M., Williams, K., Callahan, M.F., and Morris, M. (1996). Salt loading abolishes osmotically stimulated vasopressin release within the supraoptic nucleus. Neurosci. Lett. 215, 1–4.

McNamara, J.O., and Scharfman, H.E. (2012). Temporal Lobe Epilepsy and the BDNF Receptor, TrkB. In Jasper's Basic Mechanisms of the Epilepsies, 4th Ed., J.L. Noebels, M. Avoli, M.A. Rogawski, R.W. Olsen, and A.V. Delgado-Escueta, eds. (Bethesda, MD: National Center for Biotechnology Information).

Molinaro, G., Battaglia, G., Riozzi, B., Di Menna, L., Rampello, L., Bruno, V., and Nicoletti, F. (2009). Memantine treatment reduces the expression of the K(+)/Cl(-) cotransporter KCC2 in the hippocampus and cerebral cortex, and attenuates behavioural responses mediated by GABA(A) receptor activation in mice. Brain Res. 1265, 75–79.

Puskarjov, M., Ahmad, F., Kaila, K., and Blaesse, P. (2012). Activity-dependent cleavage of the K-Cl cotransporter KCC2 mediated by calcium-activated protease calpain. J. Neurosci. 32, 11356–11364.

Renaud, L.P., and Bourque, C.W. (1991). Neurophysiology and neuropharmacology of hypothalamic magnocellular neurons secreting vasopressin and oxytocin. Prog. Neurobiol. 36, 131–169.

Renaud, L.P., Jhamandas, J.H., Buijs, R., Raby, W., and Randle, J.C. (1988). Cardiovascular input to hypothalamic neurosecretory neurons. Brain Res. Bull. 20, 771–777.

Rivera, C., Li, H., Thomas-Crusells, J., Lahtinen, H., Viitanen, T., Nanobashvili, A., Kokaia, Z., Airaksinen, M.S., Voipio, J., Kaila, K., and Saarma, M. (2002). BDNF-induced TrkB activation down-regulates the K+-Cl- cotransporter KCC2 and impairs neuronal Cl- extrusion. J. Cell Biol. 159, 747–752.

Rivera, C., Voipio, J., Thomas-Crusells, J., Li, H., Emri, Z., Sipilä, S., Payne, J.A., Minichiello, L., Saarma, M., and Kaila, K. (2004). Mechanism of activity-dependent downregulation of the neuron-specific K-Cl cotransporter KCC2. J. Neurosci. 24, 4683–4691.

Sabatier, N., Brown, C.H., Ludwig, M., and Leng, G. (2004). Phasic spike patterning in rat supraoptic neurones in vivo and in vitro. J. Physiol. 558, 161–180.

Schmidlin, O., Forman, A., Sebastian, A., and Morris, R.C., Jr. (2007). Sodium-selective salt sensitivity: its occurrence in blacks. Hypertension 50, 1085–1092.

Smith, P.M., and Ferguson, A.V. (1997). Vasopressin acts in the subfornical organ to decrease blood pressure. Neuroendocrinology 66, 130–135.

Toney, G.M., and Stocker, S.D. (2010). Hyperosmotic activation of CNS sympathetic drive: implications for cardiovascular disease. J. Physiol. 588, 3375–3384.

Trudel, E., and Bourque, C.W. (2010). Central clock excites vasopressin neurons by waking osmosensory afferents during late sleep. Nat. Neurosci. 13, 467–474.

Voisin, D.L., and Bourque, C.W. (2002). Integration of sodium and osmosensory signals in vasopressin neurons. Trends Neurosci. 25, 199–205.

Yoshii, A., and Constantine-Paton, M. (2010). Postsynaptic BDNF-TrkB signaling in synapse maturation, plasticity, and disease. Dev. Neurobiol. 70, 304–322.

Zadran, S., Jourdi, H., Rostamiani, K., Qin, Q., Bi, X., and Baudry, M. (2010). Brain-derived neurotrophic factor and epidermal growth factor activate neuronal m-calpain via mitogen-activated protein kinase-dependent phosphorylation. J. Neurosci. 30, 1086–1095.